Hindawi
International Journal of Rotating Machinery
Volume 2019, Article ID 6580345, 10 pages
https://doi.org/10.1155/2019/6580345

Research Article

Effect of Rotation Friction Ratio on the Power Extraction Performance of a Passive Rotation VAWT

Jianyang Zhu[1] **and Changbin Tian**[2]

[1]*School of Machinery and Automation, Wuhan University of Science and Technology, Wuhan 430081, China*
[2]*Hubei Key Laboratory of Mechanical Transmission and Manufacturing Engineering (Wuhan University of Science and Technology), China*

Correspondence should be addressed to Jianyang Zhu; zhujianyang02@163.com

Received 27 April 2019; Accepted 24 June 2019; Published 1 August 2019

Academic Editor: Sourabh V. Apte

This paper performs a systematic numerical study to investigate the effect of rotation friction ratio on the power extraction performance of a passive rotation H-type vertical axis wind turbine (H-VAWT). In contrast to the previous literature, the present work does not impose rotation velocity on the turbine, and the rotation friction ratio which reflects the effect of external load characteristics on the turbine is introduced to the governing equation of the turbine. During each iteration, the rotation velocity of the turbine is computed after having determined the aerodynamic torque exerted on the blade of the turbine. This is more consistent with the actual working environment of the H-VAWT. A novel numerical coupling model was developed to simulate the interaction between the fluid and the passive rotation of the H-VAWT; then, the power extraction performance of the turbine with different rotation friction ratio was systematically analyzed. The results demonstrate that the power extraction performance of H-VAWT will be enhanced when the H-VAWT has appropriate rotation friction ratio. It is also found that the flow separation induced by large angle of attack is alleviated essentially if the H-VAWT has appropriate rotation friction ratio, which makes the H-VAWT have better energy extraction performance.

1. Introduction

With increasing of energy crisis and environment pollution, the performance of vertical axis wind turbine (VAWT) which is used for electricity generating has attracted a lot of interest [1]. There are three types of VAWT, named Savonius type, Darrieus eggbeater type, and Darrieus straight type [2]. Among them, the Darrieus straight type represents the most promising design for its special advantages, such as simple design, low cost, and good maintenance [3, 4]. Large numbers of computational and experimental studies have been carried out to investigate the aerodynamic performance of straight type VAWT (H-VAWT) with different parameters, and a considerable number of conclusions have been drawn [5–8].

Peng et al. [9] conducted a series of wind tunnel tests to measure aerodynamic forces on the blades of a high-solidity H-VAWT with different chord widths under different wind speeds and at various tip speed ratios, and the results showed that the high-solidity H-VAWT not only has better self-starting performance, but also possesses better power extraction performance at lower tip speed ratios. To investigate the effect of blade number on the performance of a H-VAWT, Castelli et al. [10] simulated the flow around a H-VAWT with NACA0025 airfoil, and the results indicated that with the increasing of blade number, the peak power coefficient of the turbine will decrease. Li et al. [11] conducted an experimental study to investigate the effect of Reynolds number on the power extraction performance of the H-VAWT. It was found that the higher the Reynolds number is, the better the turbine's performance possesses. Roh and Kang [12] investigated the effect of solidity on the performance of a H-VAWT by using multiple stream tube method. The results revealed that the larger the solidity is, the narrower the range of the turbine to generate positive power is. Zhu et al. [13] numerically studied the power extraction performance of a H-VAWT with utilizing synthetic jet active flow control

technique and concluded that the power extraction performance of the turbine can be enhanced by the jet effect, and the maximum increase of power coefficient is 15.2%.

Zhu et al. [14] investigated the effect of solidity and fixed pitch angle on the aerodynamic characteristics of the H-VAWT by using coupled solving incompressible Navier-Stokes (N-S) equations and passive rotation of the H-VAWT method. It was found that the solidity and fixed pitch angle influence the aerodynamic characteristics of the H-VAWT greatly, and delay stall is observed around the H-VAWT with appropriate solidity and fixed pitch angle, therefore leading the turbine to have better performance characteristics. Later, using the same method, they also studied the effect of fluctuating wind on the self-starting aerodynamic characteristics of H-VAWT, and it was concluded that the self-starting aerodynamic characteristics of VAWT will be enhanced when the fluctuating wind has appropriate fluctuation amplitude and frequency [15].

From the above aforementioned studies, it is concluded that many studies have been carried out to study the power extraction performance of the H-VAWT; however, most of the aforementioned studies consider the energy extraction characteristics of the H-VAWT with prescribed rotational speed; actually, the rotation of the H-VAWT is passive. Therefore, in this paper, we consider a H-VAWT whose rotational speed is passive and determined by the dynamic interaction between the fluid and turbine and investigate the effect of rotation friction ratio on the power extraction performance of the turbine. To this end, the rotation friction ratio which reflects the effect of external load characteristics on the turbine is introduced to the governing equation of the turbine, and a novel numerical coupling model is developed to simulate the interaction between the fluid and the passive rotation turbine. The format of this paper is organized as follows. The physical model and parameter definition are presented in section "Physical Model and Parameter Definition", followed by a description of the numerical method in section "Numerical Method". Results and discussions are presented in the next section, and some conclusions are drawn in the final section.

2. Physical Model and Parameter Definition

The object of this work is to analyze the effect of rotation friction ratio on power extraction characteristics of the 2D three blades H-VAWT. The schematic structure of the passive rotation turbine is similar to our previous published paper [14], as shown in Figure 1, where the section blade of the turbine is simplified as NACA0018 airfoil and U_∞ is the free stream velocity, ω the turbine passive rotation velocity, U_r the resultant velocity approaching to the blade section, α the angle of attack of the airfoil, θ the azimuth angle, F_t, F_n the tangential and normal force, and F_L, F_D the lift and drag force. Based on the relationship described in this figure, the angle of attack α can be defined as

$$\alpha = \tan^{-1}\left[\frac{\sin\theta}{\lambda + \cos\theta}\right] \tag{1}$$

where λ is the tip speed ratio which is defined as

$$\lambda = \frac{\omega R}{U_\infty}, \tag{2}$$

and the tangential and normal force F_t and F_n can be calculated from the equation as

$$F_t = F_L \sin\alpha - F_D \cos\alpha \tag{3}$$

$$F_n = F_L \cos\alpha + F_D \sin\alpha \tag{4}$$

Contrary to the previous literature studied on the H-VAWT, the rotation of the turbine is driven by the aerodynamic torque, which is defined as

$$Q = F_t R \tag{5}$$

According to the Newton's second law, the governing equation of the passive rotation turbine is defined as

$$J\ddot{\theta} + C\dot{\theta} = Q \tag{6}$$

where C is the rotation friction coefficient which reflects the effect of external load characteristics on the turbine, such as the resistance from the electricity generator and rotation friction between rotation shafts and bearings, and J is the inertia moment of the turbine. Then the energy absorbed from the wind is defined as

$$P_W = Q\omega \tag{7}$$

and the power coefficient is calculated by

$$C_P = \frac{P_W}{(1/2)\,\rho U_\infty^3\,(2R)} \tag{8}$$

where ρ is the wind density.

The mean power coefficient then can be described as

$$\overline{C_P} = \frac{1}{T}\int_t^{t+T} C_P dt \tag{9}$$

where $T = \omega/(2\pi)$.

There are four relative nondimensional parameters, named Reynolds number, solidity, rotation friction ratio, and density ratio to determine the fluid dynamic of the turbine. The definition of them is described as

$$\begin{aligned} Re &= \frac{2U_\infty R}{\nu}, \\ \sigma &= \frac{Nb}{2R}, \\ \psi &= \frac{C}{J}, \\ \rho^* &= \frac{\rho_w}{\rho} \end{aligned} \tag{10}$$

where ν is the fluid kinematic viscosity, N the number of the turbine, b the chord of the blade, and ρ_w the blade density.

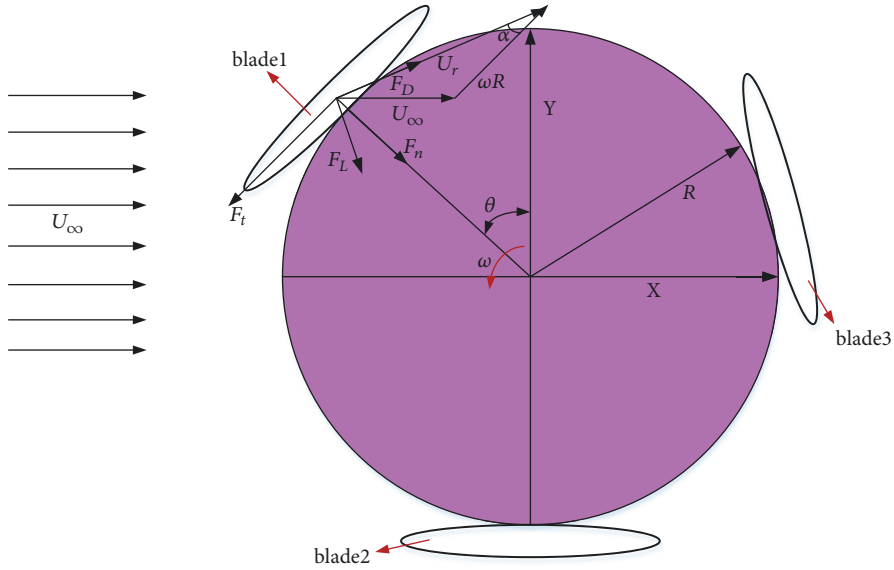

Figure 1: The schematic of the H-VAWT rotation.

3. Numerical Method

3.1. Interaction of Passive Rotation of VAWT and Fluid Solving. Considering the Reynolds number of the turbine working (at range of 10^5), it is assumed that the flow around the turbine is incompressible and turbulent; therefore, the governing equations for fluid flow are the 2-D unsteady incompressible turbulent Navier-Stokes equations:

$$\begin{aligned}
&\frac{\partial u_i}{\partial x_i} = 0 \\
&\rho\frac{Du_i}{Dt} = -\frac{\partial p}{\partial x_i} + \frac{\partial}{x_j}\left[\mu\left(\frac{\partial u_i}{\partial x_j} + \frac{\partial u_j}{\partial x_i}\right)\right] \\
&\qquad + \frac{\partial}{\partial x_j}\left(-\rho\overline{u_i' u_j'}\right) \\
&\rho\overline{u_i' u_j'} = \frac{2}{3}\rho k_v \delta_{ij} - \mu_t\left(\frac{\partial u_i}{\partial x_j} + \frac{\partial u_j}{\partial x_i}\right)
\end{aligned} \tag{11}$$

where i and j are the subscript of the velocity, u_i and u_j are the velocity vector, p is the pressure, μ is the fluid dynamic viscosity, $-\rho\overline{u_i' u_j'}$ is the Reynolds stress, δ_{ij} is the Kronecker function, k_v is the turbulent kinetic energy, and μ_t is the turbulent viscosity.

In order to solve the governing EQ (11), RNG k-ε turbulence model which is suggested for VAWT simulation by Howell et al. [16] and Almohammadi et al. [17] is employed to solve the Reynolds stress. The dynamic mesh technique is employed to simulate the passive rotation of the turbine. Meanwhile, the coupling between the pressure and the velocity is achieved by means of the SIMPLEC algorithm.

On the other hand, to solve the governing EQ (6), central difference scheme is applied for the time discretization of the passive rotation angle in EQ (6), and then EQ (6) can be rewritten as

$$\begin{aligned}
\theta_{t+\Delta t} = {} & \frac{4J}{2J + C\Delta t}\theta_t + \frac{-2J + C\Delta t}{2J + C\Delta t}\theta_{t-\Delta t} \\
& + \frac{2J}{2J + C\Delta t}\frac{Q_t}{J}\Delta^2 t
\end{aligned} \tag{12}$$

where Δt is the iteration time step and the superscript $t + \Delta t$, t and t-Δt indicate a value at the corresponding time step. $\boldsymbol{Q_t}$ is the aerodynamic torque at the current moment which can be obtained after the flow field solved.

A novel coupling method is employed to solve the interaction of fluid and passive rotation turbine. In this method, at each time step the fluid field is solved first using Ansys-Fluent to obtain the aerodynamic torque Q on the turbine, and then the passive rotation angle of the turbine under the obtained torque is determined by EQ(6), which is embedded in Ansys-Fluent using the user defined function (UDF). In the next time step, the fluid flow is solved for the turbine with an updated position angle and a new aerodynamic torque is obtained. The dynamic mesh technique is used in updating the turbine's position angle at each time step. The fluid flow and the turbine's passive rotation are solved alternatively until the turbine achieves steady cyclical rotation. For more information about the developed numerical coupling method, one can reference our previous paper [14, 15].

3.2. Mesh Generation and Boundary Conditions. A hybrid mesh system is employed, where a C type computational domain (as shown in Figure 2) contains a stationary domain and a rotating domain. Ten rows of boundary layer are used to encompass the entire blades in the rotating domain, which moves according to the turbine passive rotation, and mixed quadrilateral and triangular cells are used in the stationary

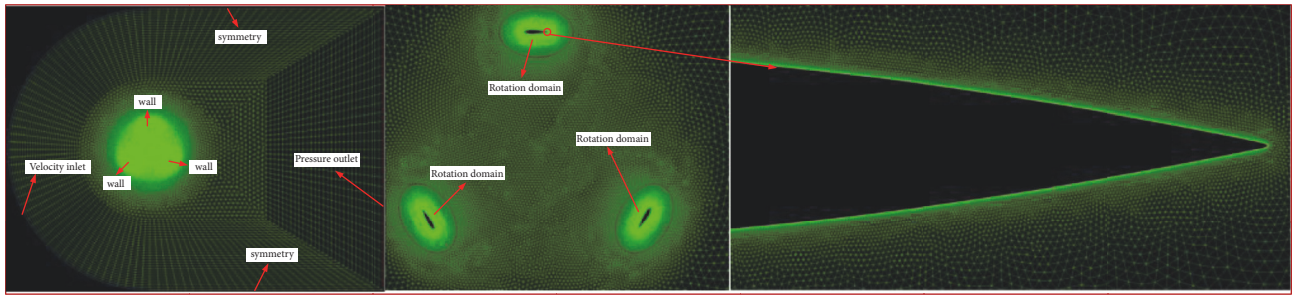

Figure 2: The mesh system with a stationary and a rotating domain.

Table 1: Details of grid numbers and iteration time steps considered in this paper.

	grid nodes on the blade	cells in the rotation zone(×3)	the height of the first cell on the blade	total number of cells	iteration time steps
grid1	200	8.5×10^3	$0.005b$	5.3×10^4	$\Delta t=1.00\times10^{-4}$ $\Delta t=1.25\times10^{-4}$
grid2	500	1.9×10^4	$0.001b$	8.6×10^4	$\Delta t=1.00\times10^{-4}$ $\Delta t=1.25\times10^{-4}$
grid3	1000	3.6×10^4	$0.0005b$	1.4×10^5	$\Delta t=1.00\times10^{-4}$ $\Delta t=1.25\times10^{-4}$

domain, where remeshing takes place at each time step. Note that in the following simulation all the y+ values on the blade surfaces are on the order of 1.0, which has been proved to be accurate for simulating the flow around VAWT by Howell et al. [16].

No-slip wall boundary condition is applied on the surface of the blade, and symmetry boundary conditions are applied on the top and also bottom computational domain. An incoming flow from left to right is applied on the left computational domain and the boundary condition is given by

$$u = U_\infty, \quad v = 0 \tag{13}$$

The pressure outlet is applied on the right computational domain and the boundary condition is given by

$$p = P_\infty \tag{14}$$

where P_∞ is the standard atmospheric pressure.

3.3. Method Validation. Firstly, computations with different grid numbers and iteration time steps are performed to ensure the independence of the numerical results on the mesh size and time-discretization scheme. Details of grid numbers and iteration time steps are shown in Table 1. These checks are carried out on the representative case of Re=3.41 × 10^5, σ=0.30, ψ=0.100, and ρ^*=75. The results of mean energy coefficient and passive rotation velocity of the VAWT for different levels of cells and time steps are shown in Figure 3. It is seen from this figure that the computation results of mean power coefficient ($\overline{C_P}$=0.075) and passive rotation velocity (ω=44.45rad/s, and results λ=3.07) have little effect by the variation of the mesh size and iteration time steps for the scheme with grid3, Δt=1.0 × 10^{-4} and grid2, Δt=1.0 × 10^{-4}. Therefore the grid3 with a number of 1.4 × 10^5 mixed cells is sufficiently dense and a size of time step 0.0001s is sufficiently small to grasp the main features of the flow around the turbine, and they are employed for the next simulations.

To ensure the reliability of the developed coupling method for simulating the interaction of fluid and passive rotation H-VAWT, we carry out the validation with a passive rotation H-VAWT model, which was experimentally studied by Hill et al. [18] and also numerically studied by Untaroiu et al. [19]. Computations are performed to compare the results with the study of Hill et al. [18] and Untaroiu et al. [19] at the same condition. The simulation parameters are Re=3.41 × 10^5, σ = 0.33, ψ = 0.0, and ρ^* = 68. The resulting passive rotation velocity is plotted against time as shown in Figure 4, where t' is defined by $t'=t/t_p$ (t_p is the time when steady rotation velocity ω was established). It is seen from this figure that the passive rotation angular velocity slightly deviates between the results of the present numerical study and that of Hill et al. when t' is at range from 0.7 to 1.0. This difference may be attributed to the neglecting of the three dimension effect and other blade supporting structures and also rotation friction for the numerical study in this work. Generally, the results of present study agree closely with that of Hill et al. [18] and Untaroiu et al. [19].

4. Results and Discussion

As conducted in Section 2, the main parameters related to the response of passive rotation H-VAWT are Reynolds number Re, solidity σ, rotation friction ratio ψ, and density ratio

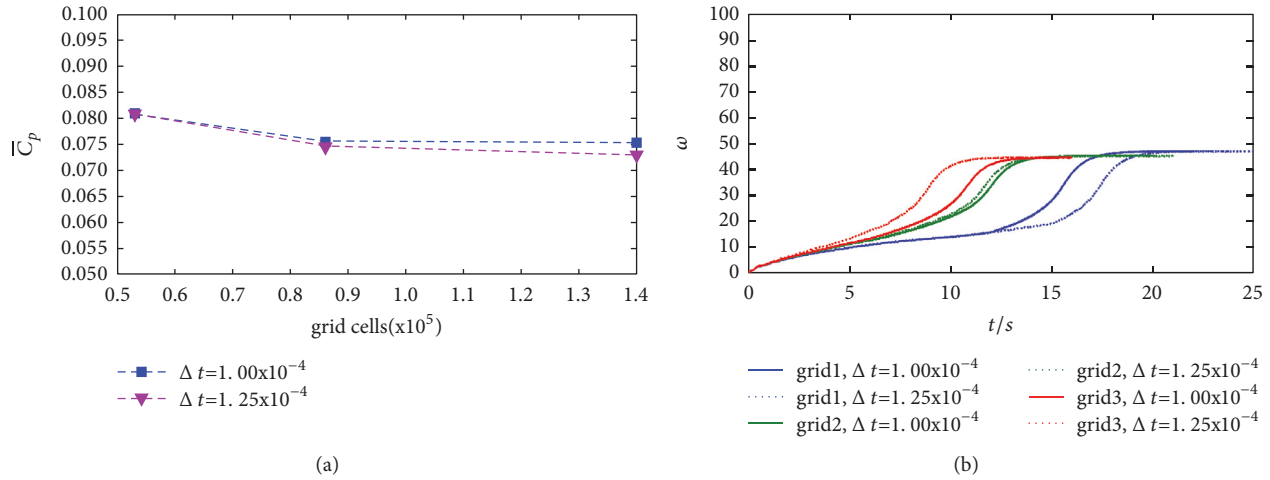

Figure 3: Evolution of mean power coefficient and passive rotation velocity of the VAWT for different levels of cells and time steps: (a) mean power coefficient and (b) passive rotation velocity.

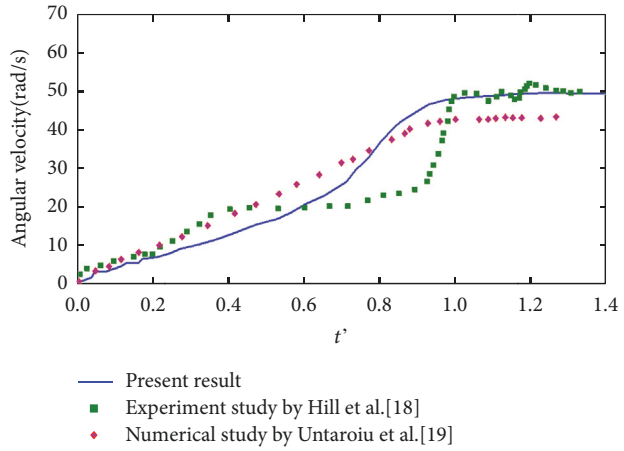

Figure 4: Time variation of the passive rotation velocity of the VAWT.

ρ^*. For the purpose of reducing the number of variables, solidity σ is fixed at 0.30 and density ratio ρ^* keeps a value of 75. Consequently, key parameters that affect the power extraction performance of the turbine are Reynolds number Re and rotation friction ratio ψ. To investigate the effect of Re and ψ on the power extraction performance of the passive rotation H-VAWT, three different Reynolds numbers Re=3.41 $\times 10^5$, 5.12 $\times 10^5$, and 6.82 $\times 10^5$ corresponding to free stream velocity U_∞ = 6m/s, 9 m/s and 12 m/s are considered, and the rotation friction ratios ψ are studied at range from 0.05 to 1.00. The other characteristic parameters of the VAWT studied in this paper are summarized in Table 2.

Table 2: Characteristic parameters of the VAWT.

Blade chord	b=0.083m
Moment of inertia	J=0.04042 kg·m^2
Rotation radius	R=5b
Wind density	ρ=1.225kg/m^3
Wind viscosity	μ=1.7894×10^{-5}
Number of blade	N=3
Blade shape	NACA0018

Figure 5 displays the mean power coefficient ($\overline{C_P}$) versus rotation friction ratio (ψ) with the considered three different Reynolds numbers. Four interesting points can be concluded from this figure. Firstly, similar variation trend of $\overline{C_P}$ with ψ is observed; no matter what value of Reynolds number does the turbine have, $\overline{C_P}$ increase first then decrease sharply with ψ, and there exists an optimal ψ where the turbine achieves the maximum $\overline{C_P}$. Secondly, as the Reynolds number increases, the value of the optimal ψ and the maximum $\overline{C_P}$ of the turbine increase. Thirdly, ψ has little influence on the $\overline{C_P}$ when ψ cross its optimal value for all the considered Reynolds number in this paper. Fourthly, for the turbine with same ψ (at range ψ<0.25), the smaller the Reynolds number is, the larger the $\overline{C_P}$ of the turbine has, which indicates that the small ψ of the H-VAWT may be of benefit for the turbine to extract

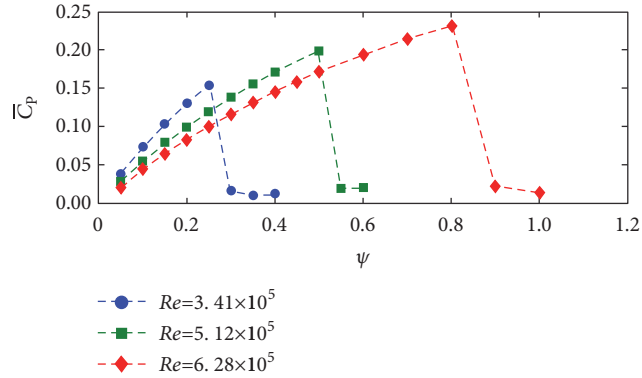

FIGURE 5: Mean power coefficient versus rotation friction ratio ψ of the passive rotation VAWT with Re=3.41 × 10^5, 5.12 × 10^5 and 6.82 × 10^5.

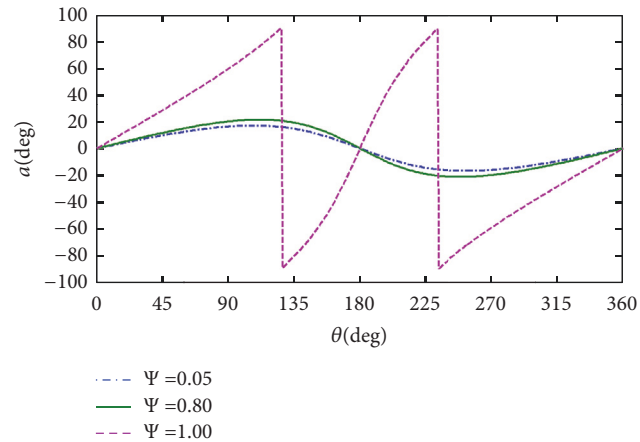

FIGURE 6: Angle of attack versus azimuth for different rotation friction ratios, at Re=6.82 × 10^5.

energy from wind under low Reynolds number, while on the contrary as the H-VAWT having larger ψ.

In order to analyze the mechanism of how the rotation friction ratio ψ affects the energy extraction characteristics of H-VAWT, three specific cases with ψ=0.05, 0.80, and 1.00 at Re= 6.82 × 10^5 are studied in detail. As conducted by Ferreira et al. [20], taking a close-up examination angle of attack of the blade during each revolution of the turbine rotor is very helpful for understanding the relative hydrodynamic behavior, such as dynamic stall. The passive rotation velocities of the turbine are 99.30rad/s, 79.25rad/s, and 17.05rad/s for the turbine with ψ=0.05, 0.80, and 1.00, respectively, which results in the turbine having tip speed ratios 3.43, 2.74, and 0.59, respectively. Figure 6 displays angle of attack of the blade1 versus azimuth for different rotation friction ratio ψ at Re= 6.82 × 10^5. The study shows that for the H-VAWT with ψ=0.05 and 0.80, angle of attack is sine-function of the azimuth angle, while for the H-VAWT with ψ=1.00, angle of attack is a sawtooth-function of the azimuth angle. Moreover, larger ψ results in high α throughout the passive rotation cycle, and the maximum amplitude of α of the H-VAWT with ψ=1.00 has value as high as 90 deg, which indicates the blade1 of the H-VAWT are in stall.

Figure 7 shows power coefficient versus azimuth angle for the three considered ψ at Re=6.82 × 10^5. Obviously, similar

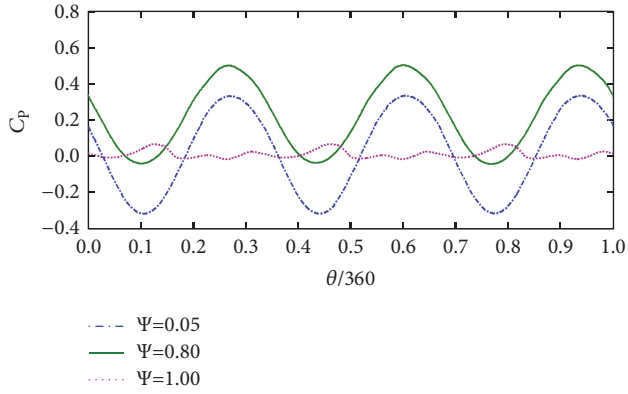

FIGURE 7: Power coefficient versus azimuth angle for the three considered ψ at Re= 6.82 × 10^5.

varying trends versus azimuth angle as angle of attack are observed. The power coefficients of the H-VAWT with ψ=0.05 and 0.80 are sine-function of the azimuth angle, while it is not for the H-VAWT with ψ=1.00. Moreover, as the ψ increase, the amplitude of C_p increases first then decreases. This finding could be explained as the angle of attack of the H-VAWT with ψ=0.05 and 0.80 is below the stall angle of

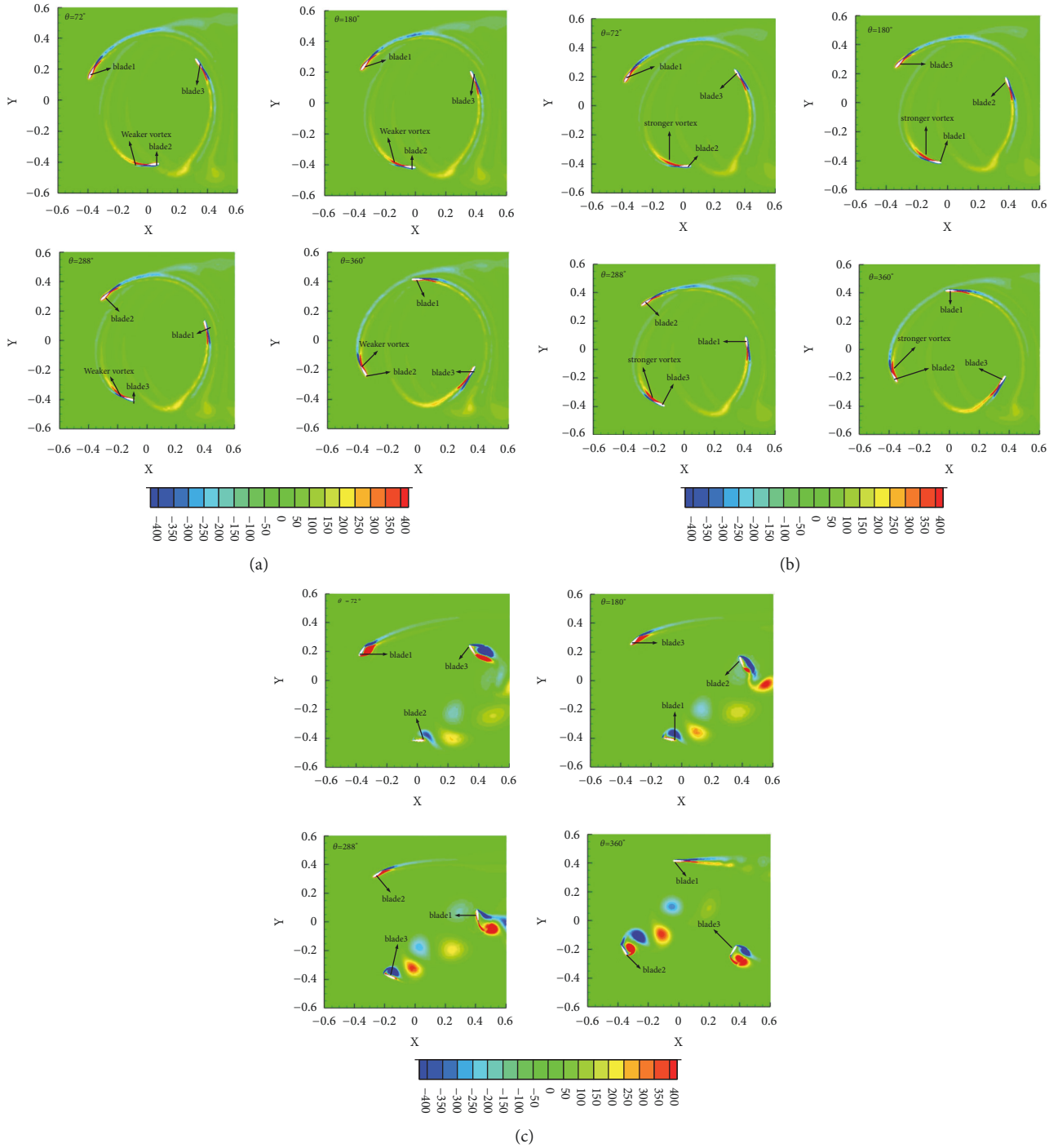

FIGURE 8: The vortices contours of the three specific H-VAWT ψ at $Re = 6.82 \times 10^5$ (a) ψ=0.05 (b) ψ=0.80 (c) ψ=1.00.

the blade at $Re = 6.82 \times 10^5$, while the angle of attack of the H-VAWT with ψ=1.00 is larger than the stall angle of the blade, which results in the H-VAWT with ψ=0.80 having larger power coefficient and the H-VAWT with ψ=1.00 having smaller power coefficient.

Figure 8 plots the vortices contours of the three specific H-VAWT considered above. It is seen from this figure that similar vortex patterns near wing surface are observed for the H-VAWT with ψ=0.05 and 0.80. During a passive rotation cycle, nearly no separated vortex is observed around the blade surface of the turbine; however, the vortex of the H-VAWT with ψ=0.80 is stronger than the H-VAWT with ψ=0.05; this finding could be explained as the angle of attack of the H-VAWT with ψ=0.80 is larger than the H-VAWT with ψ=0.05, as shown in Figure 6. On the other hand, for the H-VAWT with ψ=1.00, obviously, separated vortex exists near

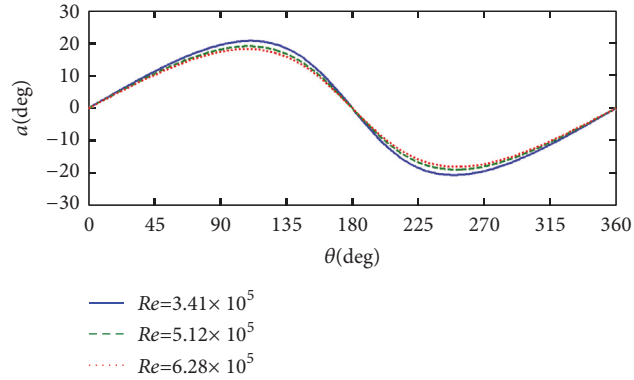

Figure 9: Angle of attack versus azimuth for different Reynolds number, at ψ=0.25.

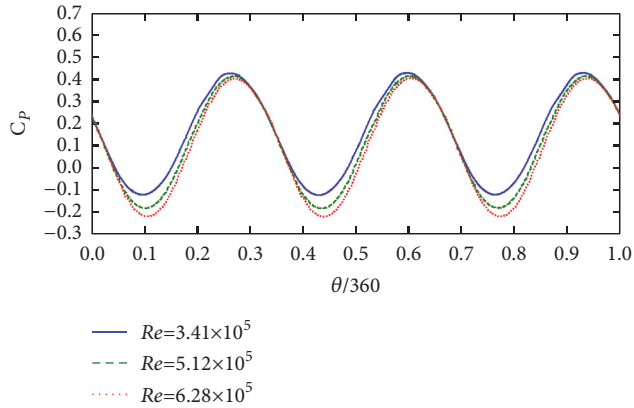

Figure 10: Power coefficient versus azimuth angle for the three considered Reynolds number at ψ=0.25.

the surface of the blade also at the flow wake of the turbine, which indicates that more energy is disappeared for the H-VAWT with ψ=1.00, which is the reason why the H-VAWT with ψ=1.00 has smallest mean power coefficient.

In order to analyze why the H-VAWT with small ψ has better power extraction performance under low Reynolds number, a specific H-VAWT with ψ=0.25 under three different Reynolds numbers considered in the last section are studied in detail. The passive rotation velocities of the turbine are 40.84rad/s, 66.40rad/s, and 92.57rad/s for the turbine with Re=3.41 × 10^5, 5.12 × 10^5 and 6.82 × 10^5 respectively, which makes the turbine have tip speed ratios 2.82, 3.06, and 3.20, respectively. Figure 9 shows angle of attack of the blade1 versus azimuth for different Reynolds numbers at ψ=0.25. It is found that angle of attack is sine-function of the azimuth angle for all the considered cases. However, lower Reynolds number results in high α throughout the rotation cycle, which is the reason why the H-VAWT at Re=3.41 × 10^5 has larger mean power coefficient, as shown in Figure 5.

Figure 10 shows power coefficient versus azimuth angle for the H-VAWT under three considered Reynolds numbers at ψ=0.25. Obviously, similar varying trends versus azimuth angle are observed; the power coefficient are sine-function of the azimuth angle. However, the positive amplitudes of the power coefficients of the turbine are almost identical, but the negative amplitudes of the power coefficients increase with the Re increasing. This finding could be explained as the angle of attack of the H-VAWT under the three considered Reynolds numbers which are all below the stall angle, while the amplitude of the angle of attack is increasing as the Re is decreasing, as shown in Figure 9, which makes the H-VAWT under low Re to have larger power coefficient and the H-VAWT under high Re to have smaller power coefficient.

Figure 11 plots the vortices contours of H-VAWT under three considered Reynolds numbers. Only two azimuth angles where the H-VAWT have peak angle of attack are considered. It is found from this figure that similar vortex patterns are observed for the H-VAWT under three different Reynolds numbers. However, the trailing vortex of the H-VAWT is close to the blade surface as the Reynolds number decreases, and the wake vortex of the H-VAWT is becoming more complex as the Reynolds number increases, which indicates that more energy disappeared for the H-VAWT under larger Reynolds number, and the delayed stall mechanism is deteriorated when the H-VAWT is under larger Reynolds number.

5. Conclusion

The object of the present study is to investigate the effect of rotation friction ratio (ψ) on the power extraction performance of a passive rotation H-VAWT. The rotation friction

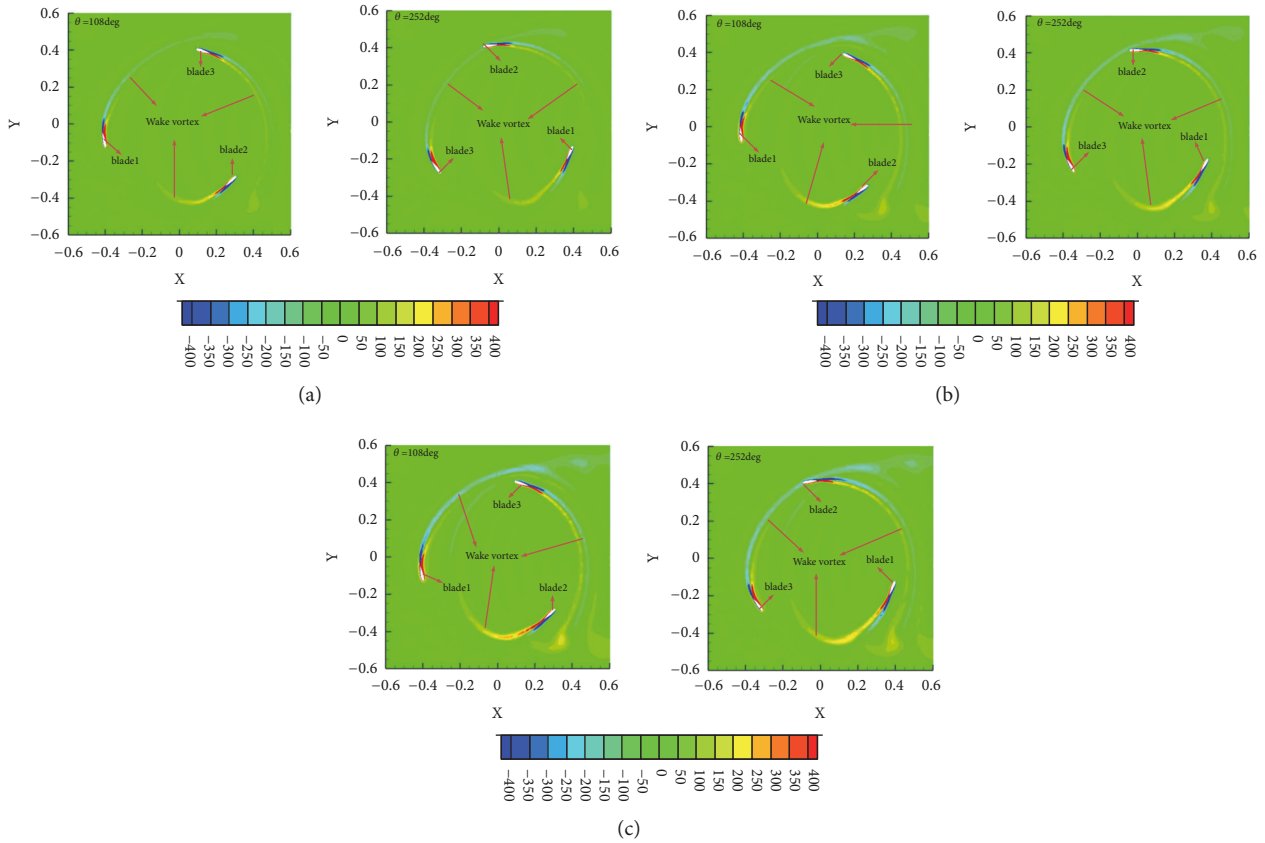

FIGURE 11: The vortices contours of H-VAWT under three considered Reynolds number at ψ=0.25, (a) Re= 3.41×10^5, (b) Re= 5.12×10^5, and (c) Re= 6.82×10^5.

ratio which reflects the effect of external load characteristics on the turbine is introduced to the governing equation of the turbine, and a novel numerical coupling model is developed to simulate the interaction between the fluid and the passive rotation turbine, and the results demonstrate that the rotation friction ratio (ψ) has significant effect on the power extraction performance of the H-VAWT. There exists an optimal ψ where the turbine achieves the maximum mean power coefficient, and the value of the optimal ψ and the maximum mean power coefficient of the turbine increase with the Reynolds number (or free stream velocity) increasing. It is also concluded that the small ψ of the H-VAWT is of benefit for the turbine to extract energy from wind under low Reynolds number, while the large ψ of the H-VAWT is of benefit for the turbine to extract energy from wind under high Reynolds number. In addition, the results from the flow field investigation illustrate that the flow separation induced by large angle of attack is alleviated essentially if the H-VAWT has appropriate ψ, which indicates that the delay stall mechanism is enhanced, therefore resulting in the H-VAWT to have better energy extraction performance. However, due to the limitation of fixed solidity and density ratio of the H-VAWT employed in the current study, more detailed physics are still being further investigated.

Data Availability

The authors are willing to share the data underlying the findings of this work, and the data used to support the findings of this study are included within the article.

Conflicts of Interest

The authors declare that they have no conflicts of interest.

Acknowledgments

This work was supported by National Natural Science Foundation of China (project No. 51505347) and key projects of the scientific research program of the Hubei Provincial Department of Education (2017CFB194).

References

[1] S. Mertens, G. Van Kuik, and G. Van Bussel, "Performance of an H-Darrieus in the skewed flow on a roof," *Journal of Solar Energy Engineering*, vol. 125, no. 4, pp. 433–440, 2003.

[2] M. Islam, D. S.-K. Ting, and A. Fartaj, "Aerodynamic models for Darrieus-type straight-bladed vertical axis wind turbine,"

Renewable & Sustainable Energy Reviews, vol. 12, no. 4, pp. 1087–1109, 2008.

[3] Y. Li, "Lecture on the technology of Vertical-axis wind turbine (III)," *Renewable Energy Resources*, vol. 27, no. 3, pp. 120–122, 2009.

[4] B. K. Kirke, *Evaluation of self-starting vertical axis wind turbines for stand-alone applications [Ph. D. thesis]*, Griffith University, Australia, 1998.

[5] A. Rezaeiha, I. Kalkman, H. Montazeri, and B. Blocken, "Effect of the shaft on the aerodynamic performance of urban vertical axis wind turbines," *Energy Conversion and Management*, vol. 149, pp. 616–630, 2017.

[6] E. Sobhani, M. Ghaffari, and M. J. Maghrebi, "Numerical investigation of dimple effects on darrieus vertical axis wind turbine," *Energy*, vol. 133, pp. 231–241, 2017.

[7] M. Zamani, M. J. Maghrebi, and S. R. Varedi, "Starting torque improvement using J-shaped straight-bladed Darrieus vertical axis wind turbine by means of numerical simulation," *Journal of Renewable Energy*, vol. 95, pp. 109–126, 2016.

[8] W. Tjiu, T. Marnoto, S. Mat, M. H. Ruslan, and K. Sopian, "Darrieus vertical axis wind turbine for power generation II: Challenges in HAWT and the opportunity of multi-megawatt Darrieus VAWT development," *Journal of Renewable Energy*, vol. 75, pp. 560–571, 2015.

[9] Y. Peng, Y. Xu, S. Zhan, and K. Shum, "High-solidity straight-bladed vertical axis wind turbine: Aerodynamic force measurements," *Journal of Wind Engineering & Industrial Aerodynamics*, vol. 184, pp. 34–48, 2019.

[10] R. M. Castelli, S. Betta D, and E. Benini, "Effect of blade number on a straight-bladed vertical-axis darreius wind turbine," *World Academy of Science, Engineering and Technology*, vol. 6, pp. 256–262, 2012.

[11] Q. Li, T. Maeda, Y. Kamada, J. Murata, T. Kawabata, and K. Furukawa, "Analysis of aerodynamic load on straight-bladed vertical axis wind turbine," *Journal of Thermal Science*, vol. 23, no. 4, pp. 315–324, 2014.

[12] S. Roh and S. Kang, "Effects of a blade profile, the Reynolds number, and the solidity on the performance of a straight bladed vertical axis wind turbine," *Journal of Mechanical Science and Technology*, vol. 27, no. 11, pp. 3299–3307, 2013.

[13] H. Zhu, W. Hao, C. Li, and Q. Ding, "Simulation on flow control strategy of synthetic jet in an vertical axis wind turbine," *Aerospace Science and Technology*, vol. 77, pp. 439–448, 2018.

[14] J. Zhu, H. Huang, and H. Shen, "Self-starting aerodynamics analysis of vertical axis wind turbine," *Advances in Mechanical Engineering*, vol. 7, no. 12, Article ID 168781401562096, 2015.

[15] J. Zhu, L. Jiang, and H. Zhao, "Effect of wind fluctuating on self-starting aerodynamics characteristics of VAWT," *Journal of Central South University*, vol. 23, no. 8, pp. 2075–2082, 2016.

[16] R. Howell, N. Qin, J. Edwards, and N. Durrani, "Wind tunnel and numerical study of a small vertical axis wind turbine," *Journal of Renewable Energy*, vol. 35, no. 2, pp. 412–422, 2010.

[17] K. Almohammadi, D. Ingham, L. Ma, and M. Pourkashan, "Computational fluid dynamics (CFD) mesh independency techniques for a straight blade vertical axis wind turbine," *Energy*, vol. 58, pp. 483–493, 2013.

[18] N. Hill, R. Dominy, G. Ingram, and J. Dominy, "Darrieus turbines: the physics of self-starting," *Proceedings of the Institution of Mechanical Engineers, Part A: Journal of Power and Energy*, vol. 223, no. 1, pp. 21–29, 2009.

[19] A. Untaroiu, H. G. Wood, P. E. Allaire, and R. J. Ribando, "Investigation of self-starting capability of vertical axis wind turbines using a computational fluid dynamics approach," *Journal of Solar Energy Engineering*, vol. 133, Article ID 041010, pp. 1–8, 2011.

[20] C. Simão Ferreira, G. van Kuik, G. van Bussel, and F. Scarano, "Visualization by PIV of dynamic stall on a vertical axis wind turbine," *Experiments in Fluids*, vol. 46, no. 1, pp. 97–108, 2009.